Pulsed RF Signal Irradiation Using a Low Voltage NLTL Coupled to a DRG Antenna *

L. C. Silva$^{\xi}$, J. O. Rossi, L. R. Raimundi, E. G. L. Rangel
National Institute for Space Research - INPE
São José dos Campos – SP, Brazil

E. Schamiloglu
University of New Mexico
Albuquerque, NM, USA

Abstract

Nonlinear Transmission Lines (NLTLs) have been used for RF generation with great success. Possible applications of NLTLs as an RF generator include aerospace radars, telecommunications, battlefield communication disruption, etc. The RF pulses generated by the NLTLs can be radiated using antennas connected to the output of the lines. Also, there has been a paucity in the literature considering experimental results on the extraction and radiation of the RF signals from the NLTL output. This work reports the results obtained with a low voltage lumped capacitive NLTL in which oscillations of about 230 MHz were produced and radiated using two Double-Ridged Guide (DRG) antennas for signal transmission and reception. The RF signal from the NLTL output was extracted using a high-pass filter decoupling circuit. The performance of the NLTL was evaluated using the analysis in time and frequency domains of the RF pulse signals at the outputs of the line and the DRG receiving antenna. A SPICE line model has been implemented showing a good agreement between the simulation and experimental results.

I. INTRODUCTION

NLTL technology has been identified as a promising source of high-power microwaves. This technology can be used as an alternative technique for pulsed high-power transmitters that includes the RF generator and the solid-state (SSA) / traveling wave tube (TWT) amplifiers [1-3]. In [4] it was demonstrated that NLTLs can generate an RF pulse with peak power of 20 MW in the 1 GHz frequency range. Other work presented the development of a high power NLTL for medical applications [5]. In this case, an antenna connected to the output of the line generates pulsed electromagnetic waves for cancer treatment.

The literature reports the practical implementation of capacitive NLTLs in which the nonlinear components are made of ferroelectric dielectrics or semiconductors that present a nonlinear behavior of their capacitance with the applied voltage. Commercially available ferroelectric materials are found in some ceramic capacitors that present a capacitance change when subjected to a great variation of voltage. The generation of high voltage oscillations using commercial ceramic capacitors is reported in [1] and [3]. The use of diodes as a nonlinear element to build NLTL has the advantage of allowing the use of commercial-off-the-shelf (COTS) components in the construction of NLTLs for producing oscillations, which can reach tens of volts for silicon varactors diodes and up to 3.3 kV for carbide silicon Schottky diodes. Furthermore, the RF propagation characteristics such as time delay, pulse width, number of oscillations, voltage modulation depth (VMD) and the line irradiation properties using broadband antennas can be easily studied in low voltage experiments.

This paper reports an investigation on the performance of a 20-section lumped capacitive NLTL. In this work, the line was driven by a 13 V input signal with a frequency of 5 MHz. The RF signal was radiated and received using two DRGs antennas. A high-pass filter was connected to the line output to extract the RF signals.

The performance of the NLTL was evaluated through time/frequency-domain analysis of the experimental results. An LT-SPICE model of this line was implemented for comparison between simulations with experimental data, showing a good agreement between both results.

II. CAPACITIVE NLTL BASIC THEORY

A capacitive NLTL uses variable capacitors as nonlinear components in parallel and inductors in series. In this experiment, a varactor diode was used as a variable capacitor (Figure 1). In this case, the capacitance of the diode varies with the applied reverse voltage.

$^{\xi}$ email: leandro@lit.inpe.br

Figure 1. NLTL circuit using varactor diodes as variable capacitors.

When the pulsed signal is applied to the input of the nonlinear line, the capacitance of the diode decreases as the pulse voltage increases. In the same way, the propagation velocity of the pulse also increases as the voltage increases. The phase velocity can be calculated using [6]:

$$v_p = 1/\sqrt{LC(V)} \qquad (1)$$

where C(V) is the variable capacitance as a function of the voltage applied across the varactor diode and L is the inductance of each section.

The NLTLs also behave as low pass filters with a cutoff frequency given by [6]:

$$f_c = 1/\pi\sqrt{LC(V\,max)} \qquad (2)$$

where C(Vmax) is the capacitance at the maximum voltage applied across the varactor diode.

Another important parameter is the characteristic impedance of the NLTL [6]:

$$Z_0 = \sqrt{L/C(V)} \qquad (3)$$

The characteristic impedance also varies with the varactor diode voltage.

III. EXPERIMENTAL SETUP AND SIMULATION MODEL

The measurements were performed on a 20-section capacitive NLTL with linear inductors of 100 nH and SVC236 varactor diodes (Figure 2). The complete varactor diode specification can be found in [7].
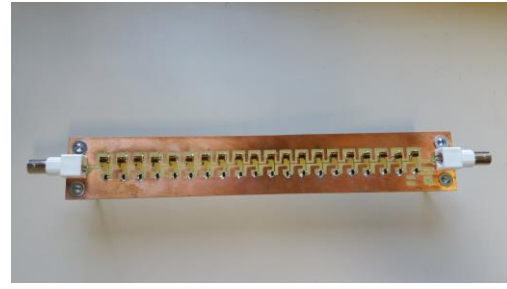
Figure 2. Photograph of the 20-section capacitive NLTL.

The first measurements were evaluated from the signal measured through the 50 Ω input of the oscilloscope. A 30-dB attenuator was connected between the line output and the oscilloscope input (Figure 3).
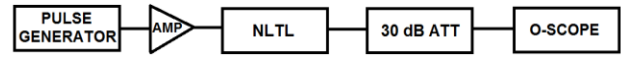
Figure 3. Block diagram of the experiment with the 50 Ω load.

The capacitive NLTL was driven by a function generator (HP 33120A) and a voltage amplifier (Apex PA98). It was supplied by a 13 V peak input signal with a frequency repetition rate of 5 MHz. A digital oscilloscope (Rohde & Schwarz RTE 1052) was used to perform the measurements (Figure 4).
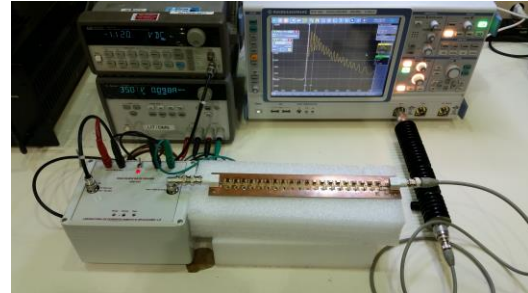
Figure 4. Photograph of the test setup.

A high-pass filter with a cutoff frequency of 200 MHz was connected to the output of the capacitive NLTL. The measurements were also evaluated from the signal measured through the 50 Ω input of the oscilloscope (Figure 5).
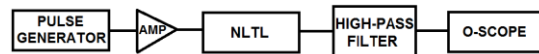
Figure 5. Block diagram of the experiment with the high-pass filter.

The basic schematic circuit with 20 sections used for the simulations using LT-SPICE is shown in Figure 6. In this model, the ohmic losses (R_L=0.3 Ω and R_D=1.0 Ω) and the self-stray capacitance of the inductors (C_P=1.5 pF) were also considered. The simulation results were compared with the corresponding experimental results.
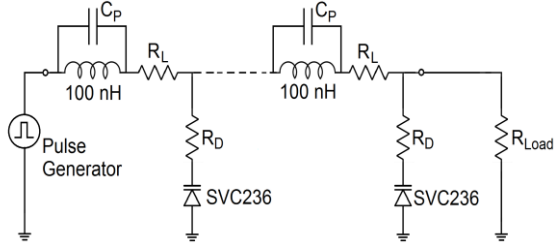
Figure 6. NLTL model for the LT-SPICE simulations.

Two Double-Ridged Guide antennas (ETS-Lindgren 3106B) were used to transmit and receive the RF pulses. The measurements were performed in an anechoic chamber to avoid electromagnetic interference (Figures 7 and 8).
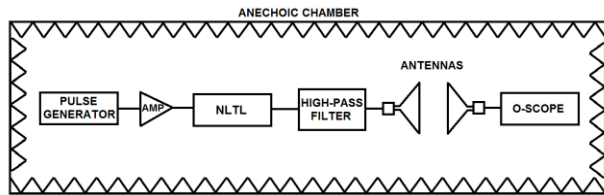
Figure 7. Block diagram of the experiment with DRG antennas.
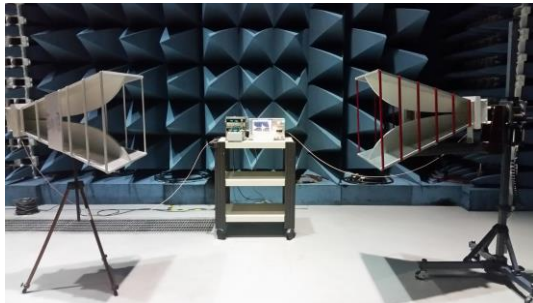
Figure 8. Photograph of the test setup in the anechoic chamber.

IV. RESULTS

The time responses of the simulation and experimental measurements with a 50 Ω resistive load, according to the test setup shown in Figure 3, are presented in Figure 9. The frequency-domain plots on decibel scales are shown in Figure 10.
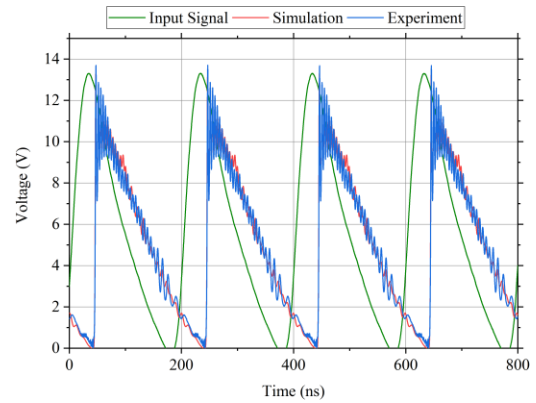
Figure 9. Time domain plots of the input pulse (experimental) and the waveforms obtained on a 50 Ω resistive load (simulation and measurement).
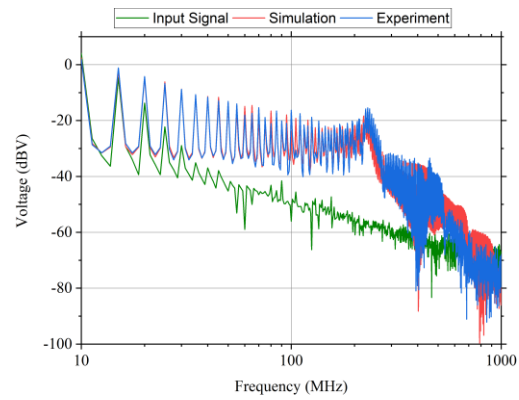
Figure 10. FFT plots of the input pulse (experimental) and the pulsed RF signal (simulation and measurement) on a 50 Ω resistive load.

The time responses of the simulation and experimental measurements with a 50 Ω resistive load when the high-pass filter is connected to the end of the line, according to test setup shown in Figure 5, are presented in Figure 11. The frequency-domain plots are shown in Figure 12.
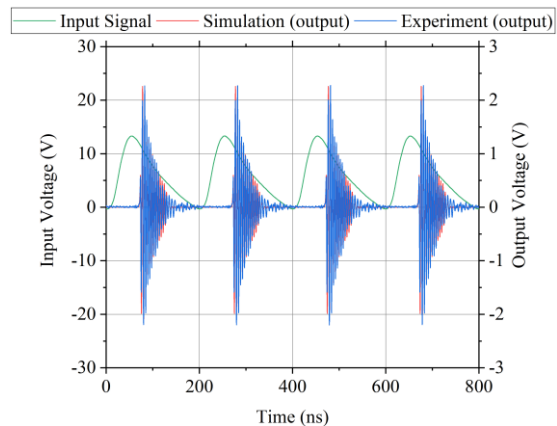
Figure 11. Time domain plots of the input pulse (experimental) and the waveforms obtained on a 50 Ω resistive load with the high-pass filter (simulation and measurement).
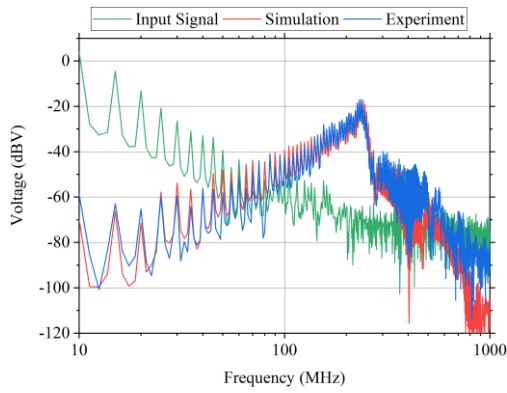
Figure 12. FFT plots of the input pulse (experimental) and the pulsed RF signal (simulation and measurement) on a 50 Ω resistive load with the high-pass filter.

The time response of the measurements of the RF signal captured by the DRG receiving antenna, according to the test setup shown in Figure 7, is presented in Figure 13. The corresponding frequency domain plot is shown in Figure 14.
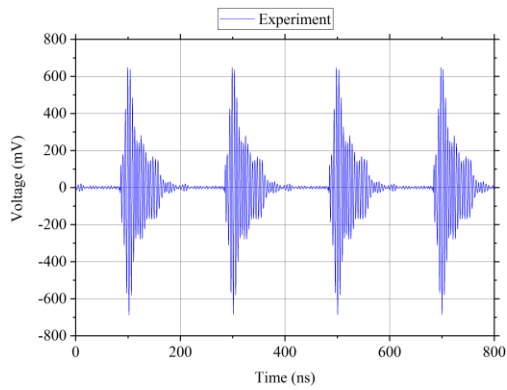
Figure 13. Time domain plot of the signal received by the DRG antenna.
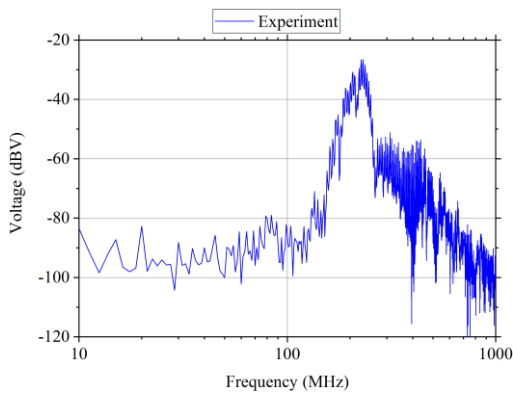
Figure 14. FFT plot of the pulsed RF signal received by the DRG antenna.

V. CONCLUSION

This paper describes an experiment with a 20-section lumped capacitive NLTL. The performance of the line was investigated focusing on different load terminations.

The experimental results and simulations showed that the oscillation frequency remains practically the same around 230 MHz for the three different cases:

1) using a 50 Ω resistive load;
2) using a high-pass filter with a 50 Ω resistive load, and;
3) using a DRG antenna as a load.

The circuit model designed for the LT-SPICE simulations was also validated against the experimental results. The RF pulses have been perfectly transmitted and received by the DRG antenna. It is expected in the future that this study can be of great interest for the design of high-power NLTLs operating at higher frequencies.

VI.   REFERENCES

[1] J. D. Darling, Paul W. Smith, "High power pulse burst generation by soliton-type oscillation on nonlinear lumped element transmission lines," in Proc. 2009 IEEE Int. Pulsed Power Conference, Washington, DC, 2009, pp. 119-123.
[2] J. O. Rossi, L. P. Silva Neto, F. S. Yamasaki, and J. J. Barroso, "State of the Art of Nonlinear Transmission Lines for Applications in High Power Microwaves," in 2013 SBMO/IEEE MTT-S, Rio de Janeiro, pp. 1-5.
[3] N. S. Kuek, A. C. Liew, E. Schamiloglu, and J. O. Rossi, "Pulsed RF oscillation on a nonlinear capacitive transmission line," IEEE Trans. on Dielectrics and Electrical Insulation, vol. 20, no. 4, pp. 1129-1135, Aug. 2013.
[4] N. Seddon, C. R. Spikings, and J. E. Dolan, "RF pulse formation in nonlinear transmission lines," in Proc. 2007 IEEE Int. Pulsed Power Conf., Albuquerque, NM, pp. 678-681.
[5] D. Yoshida, H. Ishizawa, T. Tanabe, K. Sugimoto, S.H.R. Hosseini, S. Katsuki, H. Akiyama, "Development of burst high frequency wave source for medical application," in Proc. 2013 19th IEEE Int. Pulsed Power Conf., (PPC), San Francisco, CA, 2013, pp. 1-4.
[6] P. W. Smith, "Nonlinear Pulsed Power" in Transient electronics – Pulsed Circuit Technology, John Wiley & Sons, West Sussex, England, 2002, chap. 8, p. 247.
[7] Semiconductor Components Industries, LLC, "SVC236 datasheet, monolithic dual varactor diode for FM tuning," pp. 1-6, September 1996.